A Miniaturized Circularly Polarized Antenna Using a Meandered Folded-Shorted Patch Array for CubeSats

A Miniaturized Circularly Polarized Antenna Using a Meandered Folded-Shorted Patch Array for CubeSats

Yuepei Li[1,2], Symon K. Podilchak[2], Dimitris E. Anagnostou[1]
[1]Institute of Sensors, Signals and Systems (ISSS), Heriot-Watt University, Edinburgh, UK, {yl12; d.anagnostou}@hw.ac.uk
[2]Institute of Digital Communications, School of Engineering, The University of Edinburgh, UK, {s1434099; s.podilchak}@ed.ac.uk

***Abstract*— The design and operation of a miniaturized antenna array offering circularly polarized (CP) radiation for CubeSats and other micro-satellites is presented. The proposed antenna array combines folded-shorted patches (FSPs) and meandering for antenna miniaturization. Both techniques enable a decrease of the quarter-wavelength shorted patch while maintaining a quarter-wavelength resonant length. Realization of CP is achieved by an ultra-compact and planar feed circuit consisting of a network of meander-shaped 90° and 180° hybrid couplers, providing quadrature feeding of the FSP elements and for integration onto the backside of the antenna ground plane whose physical dimension is only 9 cm x 9 cm. Good CP performances are observed for the developed UHF-band antenna for the CubeSat standard and with a size of only 0.135λ x 0.135λ considering the 450 MHz design frequency.**

***Index Terms* — CubeSats, Folded-shorted patch (FSP) antenna, sequentially rotated arrays, circular polarisation (CP), meandering, satellite communications.**

I. Introduction

Modern small satellites (MSSs) have been widely used and manufactured for earth observation, space telecommunications and geographical surveillance [1]. When compared to more conventional satellites, MSSs can significantly reduce launching costs, mission development time and make access to space more affordable [2]. One option for antenna selection is a conventional patch antenna or shorted patch. These are particularly attractive candidates due to their low cost, simple fabrication, and low profile [3]. In addition, miniaturization is possible using high dielectric constant materials; i.e. $\varepsilon_r \approx 10$. However, implementation on a CubeSat platform might not be possible given the size of the required 10 cm x 10 cm antenna footprint [4]. In addition, with antenna miniaturization, structures with optimum bandwidth (BW) and radiation efficiency are difficult to achieve.

In this work, compact and multilayer folded-shorted patches (FSPs) are investigated for the intended CubeSat antenna application. A 2 x 2 FSP antenna array offering circular polarization (CP) is presented using top-layer meandering of the folded-shorted patches as shown in Figs. 1 and 2. Element positioning and structure dimensions were optimized for antenna operation at 450 MHz. In addition, by the introduction of the meandering for the top layer of the FSP, the size of the single-element can be reduced (0.0675λ x 0.0675λ x 0.015λ) which can miniaturize the antenna element while maintaining the operational frequency. Also, the proposed antenna structure is compact in size and low-profile whilst also being suitable for the CubeSat standard.

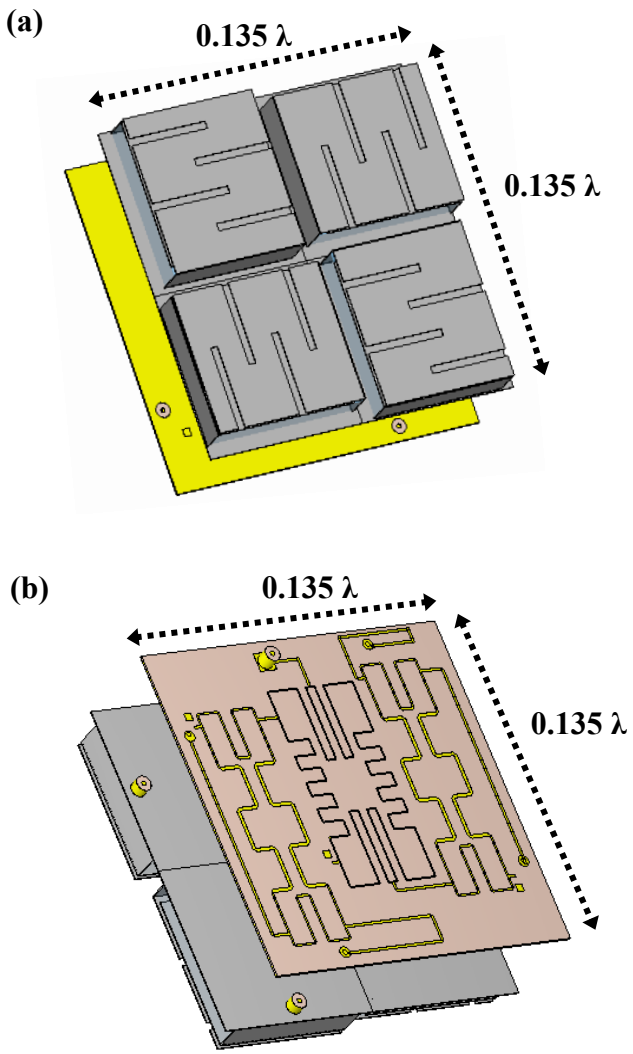

Fig. 1. Schematic of the proposed 450 MHz antenna for CubeSats: (a) 2 x 2 FSP antenna array with a 0.135λ x 0.135λ ground plane, (b) feeding system also with a total physical size of 0.135λ x 0.135λ.

In Section II of this paper, the configuration of the single-element structure and the compact feeding system are characterized. In particular, by modifying the length of the top metallic layer, the length of the meandered line as well as the position of the coaxial feed probe, antenna resonance can be tuned to optimize gain as well as achieve good 50-Ω impedance matching at the desired frequency of operation. Details of the antenna simulation results are presented in Section III while Section IV provides a brief conclusion.

TABLE I. COMPARISON TO OTHER SIMILAR FSP ANTENNAS AND ARRAYS FOUND IN THE LITERATURE CONSIDERING OPTIMIZED (SIMULATED) PARAMETERS

	Antenna Type	Number of layers	Number of Elements	Design Frequency	Reflection Coefficient	Impedance Bandwidth	Single-Element Size	Ground Plane Size	Realized Gain
[4]	Metallic & PCB	4	2x2 Array	400 MHz	< -10 dB	0.4%	0.05λ × 0.04λ × 0.05λ	0.2λ × 0.2λ	2.6 dBic
[9]	Metallic	4	Single-Element	415 MHz	-13 dB	2.9%	0.069λ × 0.065λ × 0.016λ	0.277λ × 0.277λ	—
[10]	Metallic	2	2x2 Array	400 MHz	-34 dB	5%	0.25λ × 0.25λ × 0.05λ	0.67λ × 0.67λ	6.6 dBic
This Work	Metallic & Meandering	2	2x2 Array	450 MHz	<-20 dB	0.2%	0.0675λ x 0.0675λ x 0.015λ	0.135λ × 0.135λ	1.5 dBic

II. DESIGN OVERVIEW & CONSIDERATIONS FOR THE COMPACT FOLDED-SHORTED PATCH ARRAY

Miniaturization of the conventional half-wavelength patch antenna is a topic of considerable interest within the electromagnetics community. There are several techniques for reducing the physical size of the conventional patch antenna such as the use of high relative permittivity substrates, shoring walls, meandering, capacitive loading and slots [5]-[8]. Further size reduction can be achieved by reducing the width and length of the shorting plane while also folding of the ground plane. In [9], such a linearly polarized multilayer FSP antenna was reported by increasing the number of layers to adjust the resonant frequency to 2.4 GHz, or lower frequencies realizing a single-element size of 0.13λ x 0.14λ x 0.015λ. In [10], two units of a 2 x 2 FSP array were also implemented on a small satellite body with physical dimensions of 0.5 × 0.5 × 0.5 m^3 while the operating frequency was 400MHz.

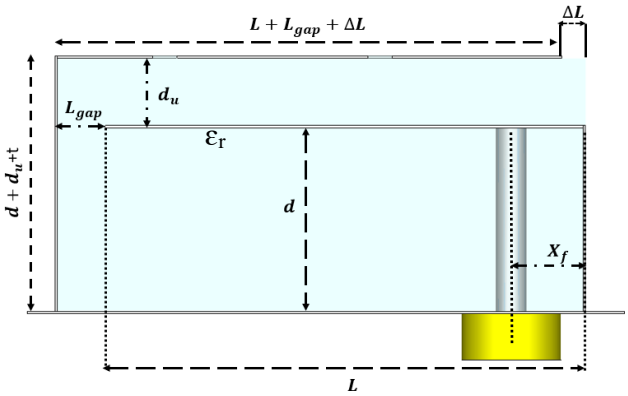

Fig. 2. Cross-sectional view of the proposed single-element, two-layer FSP antenna where the dimensions are L_{gap} = 2.5 mm, d_u = 1.5 mm, L = 42.8 mm, W = 38 mm, t = 0.3 mm, d = 8.2 mm, ΔL = 1.3 mm, and X_f = 3.1 mm. Here the top and first layers are defined at the height of $d + d_u + t$ and $d + t$, respectively.

A. Single-Element Design

The proposed FSP antenna element has been designed using a shorting wall with also a meandered top layer. This reduced the physical size of the top transmission line enabling compactness for the entire array. Also, the separation between the top and first layers was optimized for the required resonant frequency by adjusting the dimension d_u. This parameter has been varied in Fig. 3

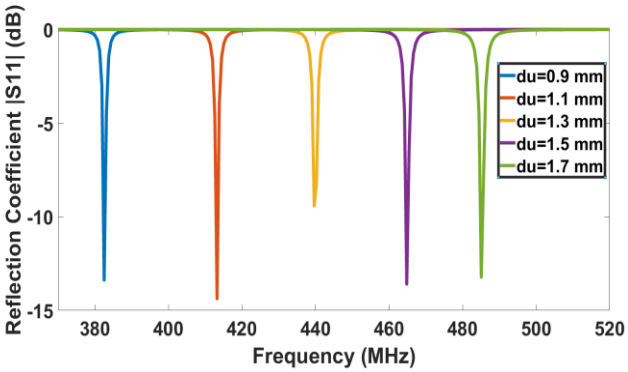

Fig. 3. Single-element $|S_{11}|$ simulations showing the possible design frequency variation by changing the dimension d_u; i.e. the height of the top layer above the first layer (see Fig. 2) while all other parameters were maintained.

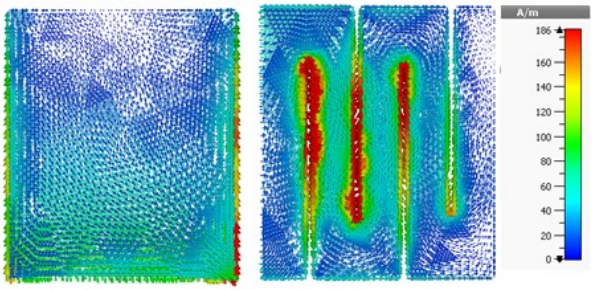

Fig. 4. Simulated surface current density at 450 MHz on top of the (a): conventional patch and (b): the meandered top patch layer. The colors for the arrows represent the current magnitude in A/m.

where it is shown that the resonant frequency can be altered for the required frequency between about 380MHz to 490 MHz for the single-element (which has the following major dimensions: 0.0675λ x 0.0675λ x 0.015λ). To the best knowledge of the authors, no similar antenna using sequential rotation for CP and meandered elements for additional compactness, has been reported in the literature (see Table I) offering comparable gain, impedance matching bandwidth, and, with reduced antenna size.

The simulated current density of the single-element FSP is also compared to a conventional patch antenna in Fig. 4. Both antennas are designed for operation at 450 MHz. It can be observed that the meandering of the top layer realized a significantly longer transmission line section, when compared to non-meandered FSP, thus, a more compact

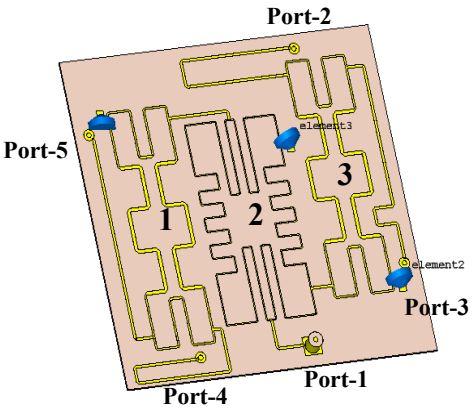

Fig. 5. Front view of the designed feeding circuit for the array to enable CP radiation. The total dimensions of the circuit are 9 cm x 9 cm (the blue elements labelled 1 to 3 are 50-Ω resistors).

antenna structure can be achieved when compared to the normal patch antenna. In these comparisons, for the non-meandered FSP (single-element) it has a physical size of 0.0735λ x 0.0735λ x 0.0163λ while the meandered FSP is 10% smaller. Also, the intense current densities between each parallel meander section can be observed in Fig. 4, which represents the open edge effects experienced by the top microstrip transmission line.

B. Generation of Circular Polarization

By using linearly polarized (LP) FSP elements and a sequentially rotated array, CP radiation can be realized [11]. In our design, each LP antenna element within the array is also fed with equal amplitude and a sequential phase shift. For example, in the most common configuration of such a 2 x 2 array, each antenna (anti-clockwise rotation) is required to have a specific phase delay of 0°, 90°, 180° and 270°. This phase delay arrangement would generate left-handed circular polarization (LHCP). For right-handed circular polarization (RHCP), similar phase shifts would be needed but with an anti-clockwise increment [11]. Also, this technique can also reduce cross-polarization levels and improve the 3-dB axial ratio bandwidth of the antenna array. Further details of the employed feeding circuit can be found in Section C.

Considering array theory, the larger the number of individual antenna elements used, the higher the antenna gain and the narrower the beam. For our work, we desire a compact antenna design with excellent radiation performances, beyond the single-element, while also maintaining a broad beam, and, by using a 2 x 2 antenna array higher gain values are expected. However, this antenna system configuration requires a feeding circuit (multi-element coupler) for bonding to the underside of the antenna ground plane whilst maintaining its low-profile and compact features.

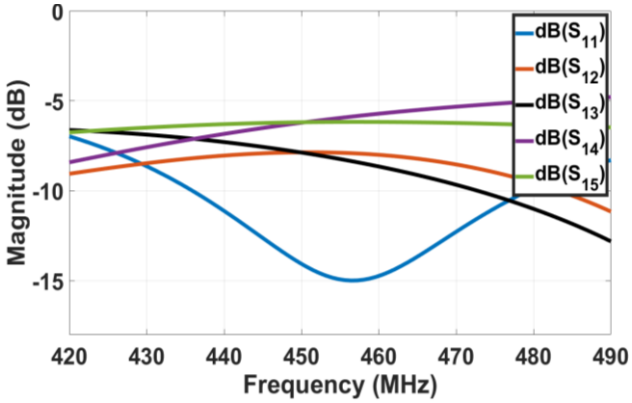

Fig. 6. Simulated magnitude of the reflection coefficient (input port) and the transmission coefficients for the feeding circuit (Fig. 5).

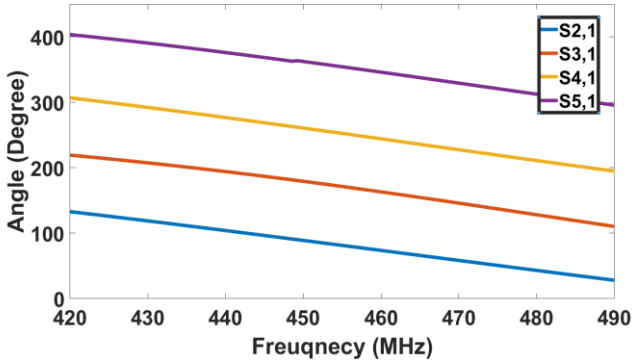

Fig. 7. Simulated phase difference in degrees between the input (Port 1) and the output (Ports 2, 3, 4, and 5) for the feeding circuit (Fig. 5).

C. Feed System Design

The proposed design of the feeding system is shown in Fig. 5. It is a 5-port network where each port provides the required 90° phase shift and with equal power splitting. Also, the feeding system employed a high permittivity material RT6010 LM (ε_r = 10.2, tanδ = 0.0023, thickness of 0.4 mm) while also using meandered microstrip sections to reduce physical circuit dimensions. By following the operation of this feeding system, port 1 can be considered the input port into the 2 x 2 array, with port 2 providing a 90˚ phase delay, port 3 providing a 180˚ phase delay, port 4 providing a 270˚ phase delay, finally, port 5 provides a 360˚ or 0˚ phase delay. Therefore, the feeding system provides sequentially rotated phase delays to the 2 x 2 FSP array for RHCP radiation.

The highlighted and numbered circuits (1 and 3, see Fig. 5) are the meandered 90˚ hybrid couplers where their physical dimensions have been reduced by more than 80% from the standard hybrid coupler whilst considering the same substrate and operating frequency. Also, the highlighted numbered 2 circuit, is the meandered rat-race coupler. The total physical dimensions for the feed system are also 9 cm x 9 cm. Simulation results for this structure suggest suitable performance; i.e. at the operating frequency of 450 MHz, the required phase shifts are achieved with $|S_{11}|$ <-14 dB. Also, the average for the output magnitudes is -7.1 dB, which defines an average insertion loss of about

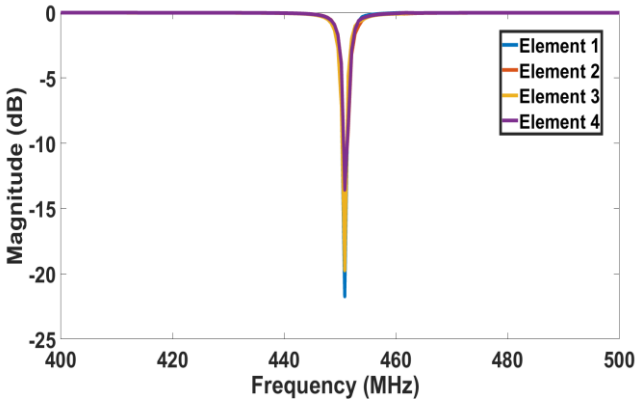

Fig. 8. $|S_{11}|$ simulation results for each antenna element showing the desired antenna operational frequency of 450 MHz for UHF applications.

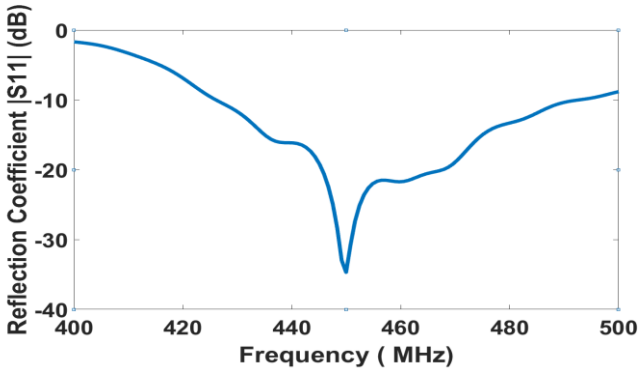

Fig. 9. $|S_{11}|$ simulation result for the complete antenna system (array and feeding circuit).

1.7 dB. This can be attributed to the value of tanδ for the employed substrate RT6010 LM. Moreover, the phase differences for each output ports are 90˚, 185˚, 265˚ and 360˚, respectively (see Figs. 6 and 7). Despite these practical concerns, the functionality of the compact feeding circuit has been demonstrated and relatively broadband performances is obtained.

III. Antenna Array Design & Results

The 2 x 2 FSP antenna array was also designed considering copper for all the required metal segments with a 0.3 mm thickness for the shorting wall as well as for the first and top layers. In addition, a 50-Ω coaxial probe feed was employed for all the individual elements at an optimized position (see the caption of Fig. 2) for best matching and realized gain at 450 MHz. Good simulated matching was also observed, as shown in Fig. 8, for each antenna element with $|S_{11}| < -15$ dB at 450 MHz (see Fig.8). In addition, a realized CP gain of 1.7 dBic was predicted by the simulation models using CST considering the complete array.

Given these simulated results, the 2 x 2 sequentially FSP array was simulated with the feeding system circuit (see Fig. 1b). For example, the coaxial probe pin for antenna element

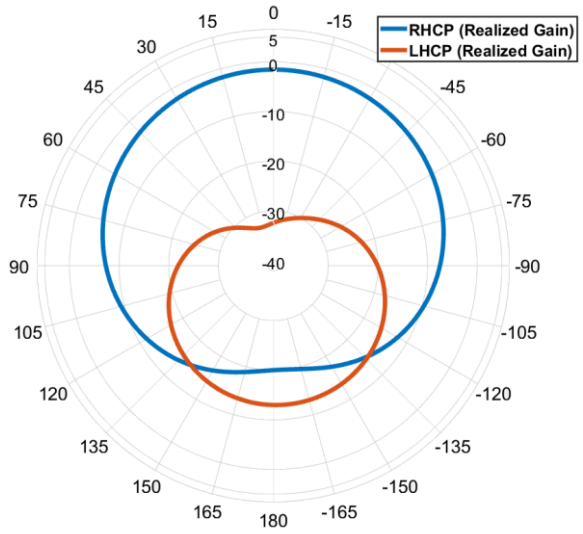

Fig. 10. Simulated RHCP realized gain pattern at 450 MHz for the compact FSP array. Results are shown along with the X-pol. levels; i.e. LHCP.

1 was connected to port 2 of the feeding system, the coaxial probe for element 2 was connected to port 3 of the feeding system, etc. This makes port 1 of the feeding circuit be the input port for the entire antenna system. In addition, the coaxial probe pins were matched to 50-Ω. It can also be observed that $|S_{11}|$ for the entire antenna system is less than -30 dB at 450 MHz (see Fig. 9).

The maximum RHCP gain was recorded to be -1.5 dBic at broadside (0˚) when the feeding circuit was included. In addition, cross-polarization levels (LHCP) are low; i.e. values are 20 dB below the main beam maximum defining axial ratios which are less than 3 dB from about +/-70° (see Figs. 10 and 11). These results are close to the previously outlined simulations, for example, the estimated RHCP gain without the feed system is about 1.5 dBic. However, as previously mentioned, there are some unavoidable losses due to the feeding circuit system as well as some extra losses which can be related to some dielectric substrate loss (tanδ) within the antenna structure as well as the transition from microstrip to the individual probes for element feeding.

Despite these practicalities, the functionality of the extremely compact antenna array and its supporting feeding circuit, which is also electrically small, has been realized demonstrating that such an antenna structure (9 cm x 9 cm) is possible for the CubeSat standard (10 cm x 10 cm x 10 cm). Also, to the best knowledge of the authors, no similar antenna structure has been reported previously for UHF operation and for integration on CubeSats. However, it should be mentioned that a very similar antenna (2-layer, 2 x 2 FSP array with top-layer meandering realizing a total structure size of 0.17λ x 0.17λ) was experimentally demonstrated in [12] for operation on picosatellites. In particular, for L-band communications between other picosatellites and more conventional satellites. For these compact picosatellite platforms (5 cm x 5 cm x 5 cm), the

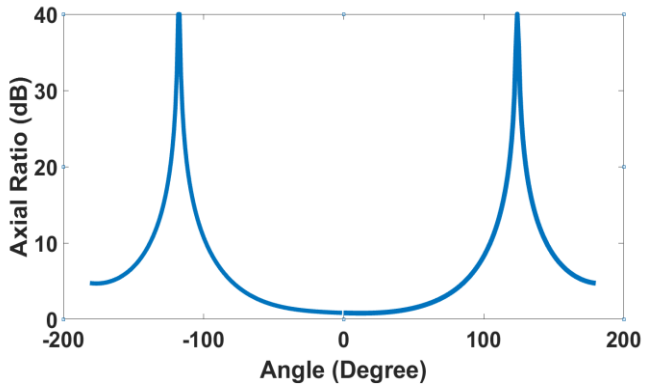

Fig. 11. Simulated axial ratio (dB) for the compact FSP array at 450 MHz.

total available layout size for the antenna is typically only about 5 cm x 5 cm or less. This defines a more compact implementation than the proposed structure of this work, albeit at higher antenna operating frequency.

IV. Conclusions

This paper investigated a miniaturized FSP antenna by using a meandered transmission line section for the top-layer enabling structure compactness. Simulation results in CST suggest that good CP realized gains and wide 3 dB axial ratio beamwidths are possible defining broad beam coverage. This is important for UHF operation at 450 MHz for CubeSat low data rate communications and other telemetry and positioning scenarios for placement onboard compact satellites [4].

The major physical dimensions for the optimized single-element was 0.0675λ x 0.0675λ x 0.015λ while the total size of the array was 0.135λ x 0.135λ x 0.015λ. A notable design challenge with such a compact array is the achieved miniaturization within an electrically small volume. In addition, RHCP polarization was achieved by the inclusion of a compact feeding system for quadrature excitation. Future work can include antenna optimization onboard a physical small satellite platform supporting any specific CubeSat mission requirements as well as design, fabrication, and assembly considering 3D printing or additive manufacturing technologies to ensure the required accuracy while also maintaining antenna efficiency and the noted CP radiation performances.

Acknowledgement

This work has been partially supported by the H2020 Marie Skodowska-Curie Individual Fellowship MSCA-IF-RI 2018 grant #840854 ViSionRF and MSCA-IF 2015 CSA-EU grant # 709372.

References

[1] H. Lokman, P.J. Soh, S. Azemi, S.K. Podilchak, S. Chalermwisutkul, M.F. Jamlos, A.A. Al-Hadi, P. Akkaraekthalin and S. Gao, "A Review of Antennas for Pico-Satellite Applications," *International Journal of* Antennas and Propagation, pp. 1 – 17, Apr. 2017.

[2] S. Gao, K. Clark, A. Sharaiha, M. Unwin, J. Zackrisson, W.A. Shiroma, J.M. Akagi, K. Maynard, P. Garner, L. Boccia, G. Amendola, G. Massa, C. Underwood, M. Brenchley, M. Pointer, and M.N. Sweeting, "Antennas for Modern Small Satellites," *IEEE Antennas and Propagation Magazine*, vol. 51, no. 4, pp. 40-56, Aug. 2009.

[3] K. F. Lee and K.-F. Tong, "Microstrip Patch Antennas", 1st ed. London, U.K.: Imperial College Press, 2010.

[4] S.K.Podilchak, M. Caillet, D.Lee, Y.M.M. Antar, L.Chu, J.Cain, M. Hammar," Compact Antenna for Microsatellite Using Folded Shorted Patches and Integrated Feeding Netwrok", IEEE Transactions on Antennas Propagation, vol. 61, no. 9, pp. 4861-4866, Sept. 2013.

[5] K. Kan So, H. Wong, K. Man Luk , C. H. Chan, Q. Xue, "A Miniature Circularly Polarization Patch Antenna Using E-Shaped Shorting Strip", Proceedings of the Fourth European Conference on Antennas and Propagation, Barcelona, 2010, pp. 1-3.

[6] S. Maci, G. B. Gentili, P. Piazzesi, and C. Salvador, "Dual-band slot loaded patch antenna," in IEE Proceedings - Microwaves, Antennas and Propagation, vol. 142, no. 3, pp. 225–232, Jun. 1995.

[7] H.K. Kan and R.B. Waterhouse, "Size reduction technique for shorted patches," *Electron. Lett.*, vol. 35, pp. 948-949, June 1999.

[8] G. A. Mavridis, D. E. Anagnostou and M. T. Chryssomallis, "Evaluation of the Quality Factor, Q, of Electrically Small Microstrip-Patch Antennas [Wireless Corner]", IEEE Antennas and Propagation Magazine, Vol. 53, Is. 4, Aug. 2011, pp. 216–224.

[9] J. Zhang, and O. Berinbjerg, "Miniaturization of multiple-layer folded patch antennas". *2009 3rd European Conference on Antennas and Propagation*, pp. 2164 – 3342.

[10] T. Debogovic, P.Robustillo-Bayon, N. Šaponjić, F. Bongard, M.Sabbadini, F. Tiezzi and J.Mosig, "Low Profile Multi-Function Antenna System for Small Satellites", *in Proc., 10th EUCAP,* 2-June, Switzerland, 2016.

[11] J. Huang, "A technique for an array to generate circular polarization with linearly polarized elements," *IEEE Transactions on Antennas and Propagation*, vol. 34, no. 9, pp. 1113–1124, Sept. 1986.

[12] Y. Li, S. K. Podilchak, D. Anagnostou, C. Constantinides and T. Walkinshaw, "Compact Antenna for Picosatellites Using a Meandered Folded-Shorted Patch Array," in IEEE Antennas and Wireless Propagation Letters, doi: 10.1109/LAWP.2020.2966088.